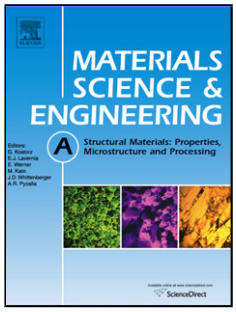

Title: The Mechanical Behaviour of an Ultrafine Grained Ti-47Al-2Cr (at%) Alloy in Tension and Compression and at Different Temperatures

Authors: V.N. Nadakuduru, D.L. Zhang, P. Cao, Y.L. Chiu, B. Gabbitas

PII: S0921-5093(11)00209-7
DOI: doi:10.1016/j.msea.2011.02.045
Reference: MSA 27113

To appear in: *Materials Science and Engineering A*

Received date: 20-10-2010
Revised date: 14-2-2011
Accepted date: 15-2-2011

Please cite this article as: V.N. Nadakuduru, D.L. Zhang, P. Cao, Y.L. Chiu, B. Gabbitas, The Mechanical Behaviour of an Ultrafine Grained Ti-47Al-2Cr (at%) Alloy in Tension and Compression and at Different Temperatures, *Materials Science & Engineering A* (2010), doi:10.1016/j.msea.2011.02.045

Research Highlights

- Powder metallurgy process has been used to produce UFG Ti-47Al-2Cr (at%) alloy.
- At room temperature, the UFG alloy was found to be ductile in compression (~ 4%).
- At elevated temperatures the alloy showed high tensile and compressive ductility.
- The yield strength at 900^{o}C is 55MPa in tension and ~ 33MPa in compression.

The Mechanical Behaviour of an Ultrafine Grained Ti-47Al-2Cr (at%) Alloy in Tension and Compression and at Different Temperatures

V. N. Nadakuduru[1], D. L. Zhang[1], P. Cao[1]*, Y. L. Chiu[2], B. Gabbitas[1]

[1]Waikato Centre for Advanced Materials (WaiCAM), Department of Engineering, University of Waikato, Private Bag 3105, Hamilton, New Zealand.

*Currently at Department of Chemical and Materials Engineering, The University of Auckland, Private Bag 92019, Auckland, New Zealand.

[2]School of Metallurgy and Materials, College of Engineering and Physical Sciences, University of Birmingham, Edgbaston, Birmingham, B15 2TT, UK.

Abstract

A bulk ultrafine grained (UFG) Ti-47Al-2Cr (at%) alloy has been produced using a powder metallurgy process that combines high energy mechanical milling (HEMM) of a mixture of Ti, Al and Cr powders to produce a Ti/Al/Cr composite powder and hot isostatic pressing (HIP) of the composite powder compact. The purpose of the present study is to determine the mechanical behaviour of the alloy in tension and compression at room temperature (RT) and elevated temperatures, and also to compare the compression behaviour of the material with its tensile behaviour. It has been found that due to the residual pores, lack of full level interparticle bonding and high oxygen content (0.87wt%) in the consolidated samples, the UFG TiAl based alloy has a very low room temperature tensile fracture strength of ~100MPa and shows no tensile ductility. However these microstructural defects and high oxygen content have much less significant effect on the room temperature compressive mechanical properties, and the alloy shows a high compressive yield strength of ~ 1410 MPa, and some ductility (plastic strain to fracture ~ 4%). At elevated temperatures of 800^{o}C and above, the alloy shows high tensile and compressive ductility as demonstrated by 75% tensile elongation to fracture and no cracking in upset forging with a height reduction of 50% at 900^{o}C. The yield strength of the alloy at 900^{o}C is 55MPa in tension and ~ 33MPa in compression, both of which are lower than those of coarse grained TiAl based alloys with similar compositions at 900^{o}C. This is due to a higher creep rate of the UFG alloy caused by the small grains. The good formability of the UFG TiAl based alloy as reflected by the lower critical temperature above which the alloy becomes highly formable indicates that the material can be used as a suitable precursor for secondary thermomechanical processing and super-plastic forming.

Keywords: Ultrafine grained, TiAl, Hot isostatic pressing, Powder metallurgy, Mechanical milling

1. Introduction

Gamma TiAl based alloys are attractive materials for aerospace and automotive applications, due to their low density, high specific strength, good corrosion resistance and attractive properties at elevated temperatures. However their wide use is limited by their low room temperature ductility and elevated temperature formability. The absence of high plasticity at fabrication temperatures is also a source of difficulties, in particular, in rolling TiAl into thin sheets or foils. Previous research has suggested that by refining the grains of the alloys to ultrafine grained (UFG) (grain sizes in the range of 100-500nm) or nanocrystalline levels (grain sizes in the range of 2-100nm) this limitation may be overcome [1-6]. However the key of realizing the promising potential of UFG and nanostructured TiAl based alloys is to develop processes and establishing optimised processing

conditions for producing high quality bulk materials containing a very low level of structural defects such as residual pores and prior interparticle boundaries that were not bonded. This can open new opportunities of using gamma TiAl based materials for making parts in a variety of automobile and aerospace applications by replacing nickel based superalloys, titanium alloys and other high temperature alloys.

During last decades, considerable efforts have been devoted to improve both the room temperature ductility and elevated temperature formability. For example γ-TAB (Ti–47Al–4(Cr, Mn, Nb, Si, B)), Ti–45Al–5.4V–3.6Nb–0.3Y and Ti–46Al–9Nb alloys with a fine grain size and good ductility have been developed [7,8]. Gerling et al. have successfully manufactured Ti–45Al–5Nb-(0,0.5)C sheets by hot rolling of blocks produced by hot-isostatic pressing of pre-alloyed powder with corresponding composition [9]. A number of studies were focussed on either the tensile behaviour or the compressive behaviour of TiAl based alloys, showing interesting and valuable results [10–13]. However the studies on both tension and compression behaviours of same TiAl based alloys and their comparison are still scarce. In this paper, we have studied both tensile and compression behaviours of UFG Ti-47Al-2Cr (at%) alloy samples at room temperature and elevated temperatures. The UFG Ti-47Al-2Cr alloy samples were prepared by a combination of high energy mechanical milling (HEMM) a mixture of Ti, Al and Cr powders to produce Ti/Al/Cr composite powder and powder consolidation using hot isostatic pressing. The study aims to achieve an in-depth understanding of the microstructural mechanisms of the mechanical properties and fracture behaviour of the ultrafine structured TiAl based alloys prepared by using the powder metallurgy route and with a substantial level of porosity and oxygen content. In the meantime, this study also elucidates the effects of temperature on the mechanical properties and fracture of such TiAl based alloys.

2. Experimental Procedure

Elemental powders of Ti (99% pure, 100 mesh), Al (99% pure, average particle size 40μm) and Cr (99% pure, -325 mesh) were first mixed for 6 hours at 100rpm without any break in a Retsch planetary ball mill to make up a powder mixture with a nominal composition of Ti-47Al-2Cr (at%). The powder mixture was subsequently milled for a total net milling time of 12 hours at a rotation speed 400rpm using the same ball mill to produce a Ti/Al/Cr composite powder. During the high energy milling stage, the ball mill was stopped for 30 minutes after every 30 minutes milling to avoid overheating of the milling vial to higher than 60^{o}C. 0.64g of stearic acid was used as a process control agent (PCA) per batch of 100g of the powder mixture. The mixing and milling were done under an inert atmosphere of high purity argon which was sealed in the vial. The Ti/Al/Cr composite powder produced by HEMM was uniaxially pressed in a die to produce a cylindrical green powder compact of 40mm in height and 34mm in diameter at a pressure of 35MPa, and the powder compacts were subsequently cold isostatically pressed (CIPed) at a pressure of 200MPa. The CIPed green powder compact was canned using 316 stainless steel tubes, and the cans were degassed by evacuating at 300^{o}C for one hour. The hot isostatic pressing (HIP) of the canned powder compact was performed at 1000 ^{o}C, for a duration of 2 hours. Dog-bone shape flat specimens with a gauge length of 16mm, a rectangle cross sectional area of 2x1mm^{2} were cut from the HIPed sample for tensile testing, while cylindrical specimens with a diameter of 6mm and a height of 10.5mm were cut from the HIPed sample for compression testing. The cutting was done using an electric discharge machining (EDM) wire cutting technique for tensile and spark electrode cutting for compression samples. The tensile testing was done at room temperature with a strain rate of 6x10^{-5}/sec and at 800 ^{o}C, 900 ^{o}C and 1000 ^{o}C, respectively, with a strain rate of 1x10^{-4} /sec, using an Instron 4240 tensile testing machine. Compression testing was done at room temperature with a strain rate of 8 X 10^{-5} /sec using the same Instron machine and at 900^{o}C with a strain rate of 1.16x10^{-4} /sec using a Gleeble thermo mechanical simulation machine, respectively. The elevated

temperature tensile testing was done under flowing argon, while the elevated temperature compression testing was done in a vacuum of $3.7x10^{-1}$ torr. The microstructures of the as-HIPed sample and tested specimens were examined using standard X-ray diffractometry (XRD), scanning electron microscopy (SEM) and transmission electron microscopy (TEM) techniques. Density measurement of the bulk alloy has been done using Archimedes principle. The oxygen content of the samples was measured to be 0.87wt% using a LECO combustion technique.

3. Results

3.1 Microstructure of the as-HIPed Sample

The XRD pattern of the as-HIPed sample (Fig. 1) showed γ-TiAl and α_2-Ti_3Al peaks being the major peaks and Ti peaks being the minor peaks. The XRD peaks were fairly broad, indicating that the grains in the sample were very fine. The density measurement showed that the as-HIPed sample had a relative density of ~ 95%. SEM backscattered electron examination of the microstructure of the as-HIPed sample showed the presence of a small fraction of Ti rich regions (bright regions in the SEM micrograph) and a substantial fraction of pores (Fig.2) which was in agreement with the relative density measurement. TEM examination of the microstructure of the as-HIPed sample (Fig. 3) showed that the microstructure consisted of equiaxed grains with sizes typically in the range of 200 - 700nm. There were also a small fraction of fairly large grains with sizes close to 1μm in diameter.

3.2 Mechanical Behaviour in Tension

Room temperature (RT) tensile testing of the specimens cut from the as-HIPed sample showed a fracture strength of approximately 100 MPa, with no sign of yielding (Fig. 4). Tensile testing of the specimens at 800°C showed an average yield strength of 85MPa, ultimate tensile strength of 90MPa and true strain to fracture of 0.4 (equivalent average elongation to fracture of 50%) (Fig. 4). As shown in Fig. 4, the specimens showed negligible strain hardening when tested at this temperature. While being tensile tested at 900°C, the specimens started yielding at a considerably lower stress, being 55MPa on average, and had an average ultimate tensile strength of 65MPa and true strain to fracture of 0.56 (equivalent average elongation to fracture of 75%). Slight work hardening was observed at this temperature (Fig. 4). The specimens tested at 1000°C were heavily oxidised under flowing argon. They showed an average yield strength of 22MPa, fracture strength of 32MPa and true strain to fracture of 0.06 (equivalent to average elongation to fracture of 8%) (Fig. 4). As shown in Fig. 4, the tensile true stress-true strain curves of the specimens tested at 800°C showed some fluctuations in stress. The reasons for such fluctuations in stress are not very clear, but it is likely that they are due to the rapid formation of new cavities in the microstructure and/or sudden increase of the moving velocity of dislocations in the TiAl grains at some points during the plastic deformation of the TiAl alloys produced using the powder metallurgy route. It is interesting to note that when the testing temperature increased to 900°C, the magnitude of fluctuations in stress became smaller (Fig. 4).

After tensile testing, the microstructure and the fracture surfaces of the tested specimens were examined to gain some understanding on how the material was deformed and fractured at different temperatures. As shown in Fig. 5, the microstructure of the room temperature tensile tested specimen resembled that of the as-HIPed microstructure. The morphology of the phase regions did not change and no noticeable amount of deformation was observed. The fracture mode of the samples tested at room temperature was quasi cleavage type, which is brittle in nature. The fracture surface showed pores (dark spots indicated by arrow A in Fig. 5(a2)) and patches of original particle surfaces which were not bonded to the neighbouring particles (dark regions indicated by

arrow B in Fig. 5(a2)). In contrast, for the specimens tested at 800 and 900°C respectively, the longitudinal sections showed that the Ti rich regions and pores were elongated indicating they were heavily sheared during tensile testing (Figs. 5(b1) and 5(c1)). For the specimens tested at 900^{o}C the direction of the Ti rich region and pore elongation was roughly at 45° to the direction of the tensile force. The fracture surfaces of the specimens tested at 800^{o}C and 900°C respectively (Figs. 5(b2) and 5(c2)) showed a fibrous type of fracture, which is ductile in nature. The sizes of the pores slightly increased with increasing the testing temperature from 800 to 900^{o}C. This is expected due to the coalescence of the residual pores.

3.3 Mechanical Behaviour in Compression

Room temperature (RT) compression testing of the specimens cut from the HIPed sample showed an average yield strength of ~ 1410MPa, a ultimate compressive strength of ~ 1640MPa, and plastic strain to fracture of ~ 4%, as shown by the compressive engineering stress-engineering curves (Fig. 6(a)). At the end of the compression testing, the specimens were broken into multiple pieces, making a loud sound. The specimens used in RT compression testing and the pieces produced from the RT compression testing are shown in Figs. 6(b) and (c), respectively. Compression test of the specimens cut from the as-HIPed sample at 900^{O}C showed that the specimens had an average compressive yield strength of 33MPa (Fig. 7(a)). The specimens were deformed to a true strain of ~ 0.7 (equivalent to a height reduction of 50%) without cracking or fracturing (Fig. 7 (b)), and the compression test was stopped at that point. The specimens exhibited a bell shape after testing, showing that the plastic deformation of the specimen was not uniform during compression. Strain hardening was observed during the compression testing, as shown in Fig. 7(a). The observation of the cross section of a specimen which was compressed at RT until the load approached the maximum load but prior to fracturing revealed that the fraction and sizes of pores (or cavities) increased dramatically during the RT compression testing (Fig 8(a)). On the other hand after elevated temperature compression testing almost all the pores was closed, and the shape of remaining pores changed to spherical (Fig 8(b)). The fracture surface examination of the RT compression tested specimens revealed that the fracture was mainly quasi cleavage type which is brittle in nature (Figs. 9(a) and (b)). However a few regions of the fracture surface showed fibrous morphology (Figure 9(c)), indicated that in some regions significant plastic deformation occurred at a microscopic scale.

4. Discussion

4.1 Room Temperature Mechanical Behaviour

The as-HIPed Ti-47Al-2Cr alloy in the present study has a high level of porosity (~ 5%) and a low level of interparticle bonding, indicating that the full level of consolidation is not achieved. The high level of porosity and low level of interparticle bonding show that the temperature and time used for the HIP experiment are not sufficient to achieve a fully dense bulk material. On the other hand the high oxygen content of the consolidated sample (0.87wt%) is due to the high oxygen content of the as-milled Ti/Al/Cr powder used (0.7wt%) and perhaps also the relative low temperature (300^{o}C) used for degassing of the powder compacts which is not sufficient to eliminate all the volatiles absorbed onto the particle surfaces. The room temperature tensile behaviour is strongly influenced by the low level of consolidation. The pores and interparticle boundaries without bonding can act as crack initiation sites at a fairly low tensile stress, and since the γ-TiAl phase has low ductility by nature, premature fracture of the bulk material can occur at a low tensile stress which is much lower than the yield strength of the alloy. The high oxygen content of the bulk sample makes the material very brittle, which further increases the possibility of premature fracture

of the tensile test specimens. Both of these factors cause the average measured tensile fracture strength of the specimens to be very low (~100MPa).

While in compression the samples showed yielding with an average yield strength of 1410MPa which is comparable to that of UFG γ-TiAl alloys with similar compositions and grain sizes [14] and significantly higher than that of coarse grained γ-TiAl alloys with similar compositions [13]. However Oehring et. al [15] has demonstrated a strength of 2500MPa for an UFG TiAl alloy with a similar composition but smaller average grain size and the alloy was found to be brittle in compression. According to Brace et. al [16], there are three modes of crack initiation and propagation in compression: crack initiates and propagates along the compression axis (Fig. 10(a)); crack initiates at a triple grain junction and propagates along the grain boundary that is parallel to the compression axis (Fig. 10(b)); and two cracks initiate and propagate at both ends of an inclined precrack, which is produced along a grain boundary which is inclined with respect to the compression axis. According Cao et. al [17] the fracture modes of TiAl alloys in compression can take both shear and cleavage fractures depending on the crack initiation and propagation mode. The fracture of the TiAl alloy specimens in compression may occur in the same way, as suggested by the fracture surface shown in Figs. 9(b) and (c) which show that the fracture is cleavage on macroscopic scale and ductile at microscopic level. As shown in Fig. 8(a), there are many pores in the specimens under a compression load, close to the fracture load of the material. This means that a lot of cracks are initiated simultaneously and rapid fracture can occur by connecting the numerous microcracks in the specimen. It should be pointed out that a substantial fraction of those pores shown in Fig. 8(a) are caused by the easy separation of the powder particles at interparticle boundaries which are lack of bonding. It is expected that the original residual pores in the HIPed samples and the pores formed under high stress prior to fracture makes the UFG TiAl alloy sample have a lower ductility in compression than the coarse grained TiAl alloy with a similar composition [13]. In addition, the unreacted Ti regions found in the microstructure of the HIPed samples are also expected to adversely affect the room temperature mechanical properties (especially the ductility) due to their brittleness caused by the high total oxygen content of the HIPed sample. It is well known that titanium has a much higher solubility for oxygen than TiAl phase, so the oxygen content in Ti regions can be much higher than the average oxygen content of the HIPed sample which is 0.87wt%. This high oxygen content in Ti regions can make them very brittle and thus can more effectively cause premature fracture of the tensile test specimens at room temperature and reduce the compressive ductility of the alloy. It is not certain how the unreacted Ti region would affect the mechanical properties of the HIPed sample at 800^{o}C and above due to the high tolerance of the material to dissolved oxygen in terms of plastic deformation, but it can be expected that the unreacted Ti would have less effect.

4.2 Elevated Temperature Mechanical Behaviour

Figs. 11 and 12 show the yield strength of the UFG Ti-47Al-2Cr alloy prepared in this study and several TiAl based alloys with similar compositions in tension and compression, respectively. From Fig. 11, it can be seen that the tensile yield strength of the UFG Ti-47Al-2Cr alloy at 800^{o}C is significantly lower than that of the UFG Ti-47Al-3Cr alloy with a smaller average grain size [18] (180nm vs ~600nm) and that of the coarse grained Ti-47Al-2Cr-0.2Si alloy [19]. In the meantime, the tensile yield strength of the UFG Ti-47Al-3Cr alloy is also substantially lower than that of the coarse grained Ti-47Al-2Cr-0.2Si. This shows that both reduction of grain size and the presence of pores may lower the yield strength at 800^{o}C. The strength of the UFG Ti-47Al-2Cr alloy at 900 and 1000^{o}C is very comparable to that of UFG Ti-47Al-3Cr alloy, showing that the presence of pores in the original samples and the small difference in grain size does not affect the tensile yield strength of the alloy at 900 and 1000^{o}C. From Fig. 12, it can be seen that the compressive yield strength of the UFG Ti-47Al-2Cr alloy at 900^{o}C is the same as that of the UFG Ti-48Al alloy, and the

compressive yield strength of both alloys at this temperature is clearly lower than that of the coarse grained Ti-47Al-2Cr-0.2Si alloy. This shows that the presence of porosity has very little effect on the compressive yield strength of the alloy at 900^{o}C, but the very small grain size reduces the compressive yield strength. The observation that the yield stresses of TiAl based alloys at temperatures above 800^{o}C are lower as compared to those of their coarse grained counterparts at the same temperatures is in agreement with the observation made by Yan et al. [20]. According to Bohn et al [14] and Oehring et al [15, 21] the mechanisms of creep of TiAl based alloys at elevated temperatures are dislocation climb and grain boundary sliding (GBS) facilitated by atomic diffusion. Grain boundary sliding is expected to occur above 1000^{o}C for coarse grained TiAl based alloys, while this mechanism can be one of the dominant mechanisms of creep at temperatures well below 1000^{o}C for UFG TiAl alloys. This can reasonably explain the observation that the UFG TiAl based alloys have lower yield strengths than the coarse grained TiAl alloys with similar composition at 800 (for both tension and compression), 900 and 1000^{o}C (for compression), respectively.

The fracture surfaces of the tensile test specimens tested at 800 and 900^{o}C (Figs. 5(b2) and 5(c2)) showed large cavities and small dimples. The large cavities are the pores present in the specimens as revealed by examining the longitudinal section of the tested specimens (Fig. 5(b1) and 5(b2)). It has been observed that the pores size slightly increased as the testing temperature increased. This behaviour is similar to that observed in other studies [14,22]. It can be understood that cavities formed during elevated temperature tensile testing is due to four reasons: a) residual pores; b) improper accommodation of the shear strains; c) thermally induced pores (TIP) due to entrapped gas inside the bulk material; and d) separation of particles at interparticle boundaries without bonding. However the role of the entrapped gas depends on the processing technique used. In the case of forging it results in internal cracks, while for HIPed samples it results in blow holes. It is known that TiAl alloys prepared using a powder metallurgy route are more prone to cavitation behaviour mainly due to thermally induced pores and in some cases residual pores. However for the alloys prepared in ideal conditions and with no microstructural defects only two types of cavitation behaviour may be expected, which can be either from TIP or improper accommodation of sliding strain. Also it is known fact that reducing the grain size is used as a counter measure to reduce cavitation [14,22], so the increase in pore size observed in the Ti-47Al-2Cr alloy with the grains at UFG level can be mainly attributed to the residual pores and opening up of non bonded interparticle boundaries.

It has been observed in the present study that despite the fairly high oxygen content (0.87wt%) of the bulk Ti-47Al-2Cr alloy, its formability at 900^{o}C is very good, as demonstrated by the high tensile elongation to fracture (75%) and absence of cracking during upset forging with a height reduction of 50% in the compression test. This behaviour of the TiAl based alloy is similar to that observed for UFG TiAl alloys reported in literature [15, 23]. This confirms that the critical temperature above which the UFG Ti-47Al-2Cr alloy becomes highly formable is much lower than that of the coarse grained TiAl alloys with similar compositions [24-26]. As discussed above, this difference in formability between UFG and coarse grained TiAl based alloys can be attributed to higher creep rate of UFG alloys at a given elevated temperature due to their fine grains.

The mechanical properties of the Ti-47Al-2Cr alloy investigated in this study can be improved by several methods which can lead to reduction of the level of porosity and improvement of the level of bonding between powder particles. The methods include either increasing the HIP time or HIP temperature and secondary thermomechanical processing of the as-HIPed samples such as forging and rolling. On the other hand reduction of the oxygen content in the as-milled powder by avoiding the use of process control agent in HEMM and minimising the content of volatiles in the powder compact by using better degassing procedure before sealing the can are critical for improving the quality of the consolidated material. The high ductility of the consolidated alloy samples at elevated temperatures despite their high porosity level and high oxygen content suggests that the hot

formability of the material for secondary processing is very high, leaving a large space for improvement of the quality and microstructure of the alloy through secondary thermomechanical processing.

5. Conclusions

A bulk ultrafine grained (UFG) Ti-47Al-2Cr alloy of average grain size of ~ 600nm has been produced using a combination of mechanical milling and hot isostatic pressing. It is confirmed that the microstructural defects such as pores, low interparticle bonding and high oxygen content in the as-HIPed material are less significant in affecting room temperature compression behaviour as compared to that in tension. A high yield strength of ~ 1410 MPa, and plastic strain to fracture ~ 4% are observed in compression at room temperature. At elevated temperatures of 800^{o}C and above, the alloy showed high ductilities both in tensile and compressive deformations as demonstrated by 75% tensile elongation to fracture and no cracking in upset forging with a height reduction of 50% at 900^{o}C. The yield strength of the alloy at 900^{o}C is 55MPa in tension and ~ 33MPa in compression, which are found to be lower than those of coarse grained TiAl based alloys with similar compositions at 900^{o}C. The high formability of the Ti-47Al-2Cr alloy at elevated temperatures despite the high porosity and low level of interparticle bonding revealed that the material can be used as a suitable precursor for secondary thermomechanical processing and super-plastic forming.

Acknowledgements
The authors would like to thank the Foundation for Research, Science and Technology (FRST), New Zealand for the financial support to the research work presented in this paper.

References

1. V.Y. Gertsman, M. Hoffmann, H. Gleiter and R. Birringer, Acta Metallurgica et Materialia, 1994. 42: p. 3539.
2. P.G. Sanders, J.A. Eastman and J.R. Weertman, Acta Materialia, 1997, 45: p. 4019.
3. R. Bohn, G. Fanta, T. Klassen and R. Bormann, Scripta Materialia, 2001, 44: p. 1479.
4. Koch. C.C. , Morris. D.G. , Lu. K., Inoue. A, MRS Bulletin**,** 1999, 24: p. 54.
5. R. Bohn, T. Klassen and R. Bormann, Acta Materialia, 2001, 49: p. 299.
6. Li XIA, Hui DING, Xuefong Ruan and Yaoyao REN, Rare Metals, 2007, 26: p. 572.
7. Rainer Gerling, Arno Bartels, Helmut Clemens, Heinrich Kestler and Frank-Peter Schimansky, 2004, 12: p.275.
8. Y.Y. Chen, F. Yang, F.T. Kong and S.L. Xiao, Journal of Alloys and Compounds, 2010, 498: p. 95.
9. R. Gerling, F.P. Schimansky, A. Stark, A. Bartels, H. Kestler, L. Cha, C. Scheu and H. Clemens, Intermetallics, 2008: p. 16.
10. K. S. Chan and Y. W. Kim, Metallurgical and Materials Transactions A, 1992, 23A: p.1663.
11. K. S. Chan Metallurgical and Materials Transactions A, 2000, 31A: p.71.
12. C.T. Liu, J.H. Schneibel and P.J. Maziasz, Intermetallics, 1996, 4: p. 429.
13. K. Nonaka, K.Tanosaki, M. Fujita, A. Chiba, T. Kawabata and O. Izumi, Materials Transactions, JIM, 1992. 33: p. 802
14. R. Bohn, T. Klassen and R. Bormann , Intermetallics, 2001. 9: p. 559.
15. M. Oehring, F. Appel, Th. Pfullmann, and R. Bormann, Applied Physics Letters,1995. 66: p. 941.
16. W.F. Brace, B.W. Paulding and C. Scholz, Journal of Geophysics *Research*, **71** (16) (1966), pp. 3939–3953.

17. R. Cao, L. Li, J.H. Chen and J. Zhang, Materials Science and Engineering A, 2010, **527**, 2468.

18. M. R. Shaigev, O.N. Senkov, G. A . Salishchev, F. H. Froes, Journal of alloys and compounds, **313,** 201.

19. H. Clemens, W. Glatz and F. Appel**,** Scripta Materialia, 1996. **35**: p. 429-434.

20. Y. Q. Yan, Z. Q. Zhang, G. Z. Luo, K. G. Wang and L.Zhou, Materials Science and Engineering A, 2000. **280,** 187.

21. M. Tokizane, Y. Takaki, and K. Ameyama, Metal Powder Industry Federation, Princeton, NJ, 1992, 7, 315.

22. G. Wegmann, R. Gerling, F. P. Schimansky, H. Clemens, A. Bartels, Intermetallics, 2002. 10, 511.

23. H. Yu, D. Zhang, Y.Y. Chen, P. Cao, B. Gabbitas, V. Nadakuduru, Proceedings of Ti-2007 Science and Technology, The Japan Institute of Metals (2007), Sendai, Japan, pp. 667-670.

24. J. Beddoes, Material Science and Engineering A, 1994. **184,** L11**.**

25. H. Y. Kim, W. H. Sohn, S. H. Hong, Material Science and Engineering A, 1998. **251**, 216.

26. Appel F, Lorenz U, Sparka U, Wagner R, Proc. of the 10th Int. Conference ICSMA 10. Sendai, Japan: JIM, 1994. p. 341.

Figure Captions

Fig. 1: XRD pattern of the as-HIPed Ti-47Al-2Cr alloy sample (CuK_α , $\lambda = 1.5418$ Å).

Fig. 2: SEM backscattered electron image of the as-HIPed sample showing the distribution and sizes of the Ti rich regions (bright regions) and the pores.

Fig. 3: (a) and (b) Bright field TEM images of the microstructure of the as-HIPed sample.

Fig. 4: Tensile true stress-true strain curves of the specimens tensile tested at (a) room temperature (b) 800°C (c) 900° C (d) 1000°C.

Fig. 5: SEM backscattered electron images of the longitudinal sections (within gauge length) ((a1), (b1) and (c1) and corresponding SEM secondary electron images of the fracture surfaces of the tensile tested specimens ((a2), (b2) and (c2)) tested at different temperatures: (a1) and (a2) room temperature; (b1) and (b2) 800°C; and (c1) and (c2) 900°C.

Fig. 6: (a) The compressive true stress-true strain curve of a specimen tested at room temperature; (b) image of the specimens used for room temperature compression testing; and (c) fractured pieces after room temperature compression testing.

Fig. 7: (a) The compressive true stress-true strain curve of a specimen, tested at 900°C; (b) specimens after compression testing at 900°C.

Fig. 8: Images of the cross sections of the specimens after compression testing at (a) room temperature and (b) 900°C (arrows indicate direction of the compressive force)

Fig. 9: Fractured surfaces of the specimens after RT compression testing, showing (a) quasi cleavage type of fracture; (b) quasi cleavage with a few regions showing ductile fracture behaviour; (c) a region of ductile fracture.

Fig. 10: Crack initiation and propagation paths in compression loading mode [17, 18]

Fig. 11: Comparison of yield strength in tension of TiAl based alloy samples of similar compositions at different temperatures.

Fig. 12: Comparison of yield strength in compression of TiAl based alloy samples of similar compositions at different temperatures.

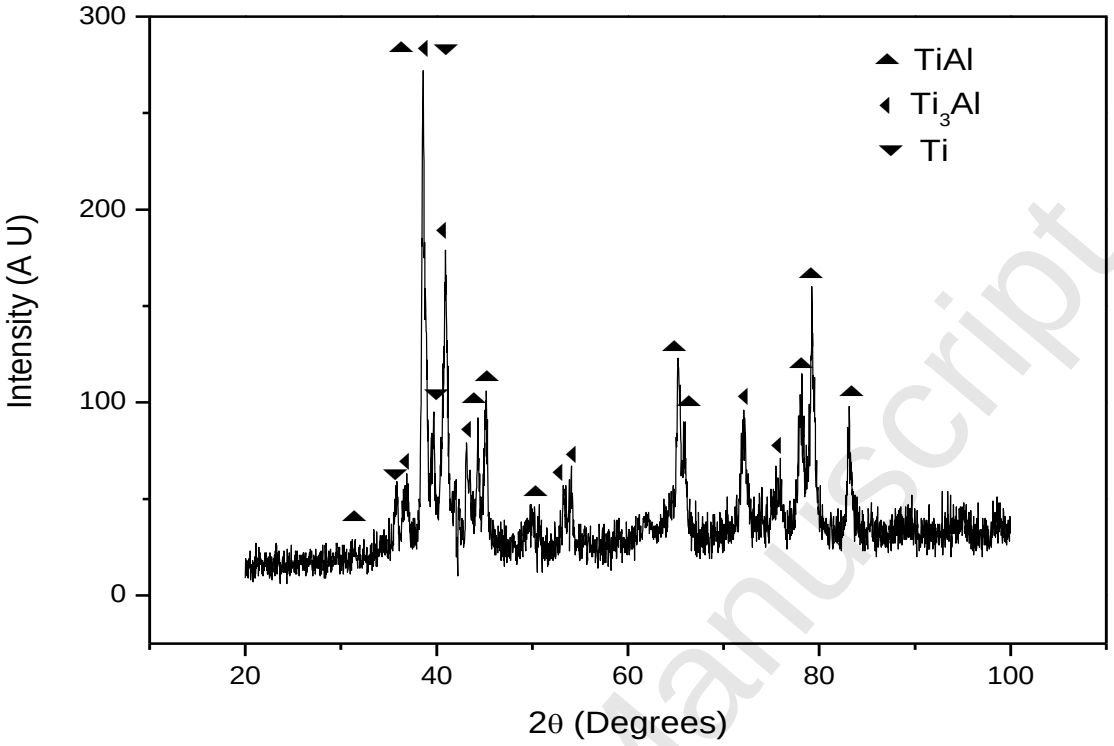

Fig. 1: XRD pattern of the as-HIPed Ti-47Al-2Cr alloy sample (CuK_{α} , $\lambda = 1.5418$ Å).

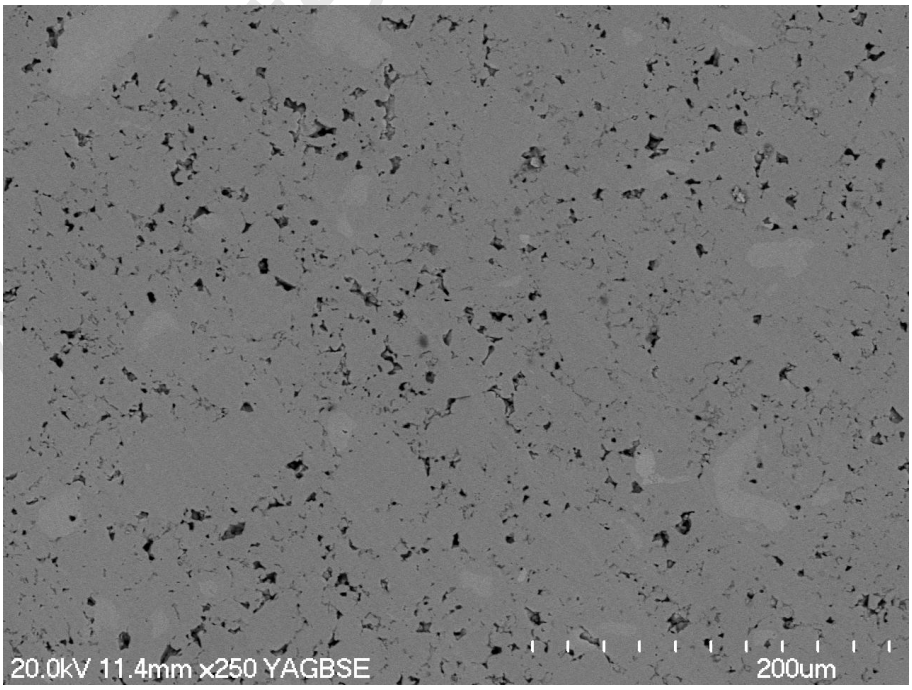

Fig. 2: SEM backscattered electron image of the as-HIPed sample showing the distribution and sizes of the Ti rich regions (bright regions) and the pores.

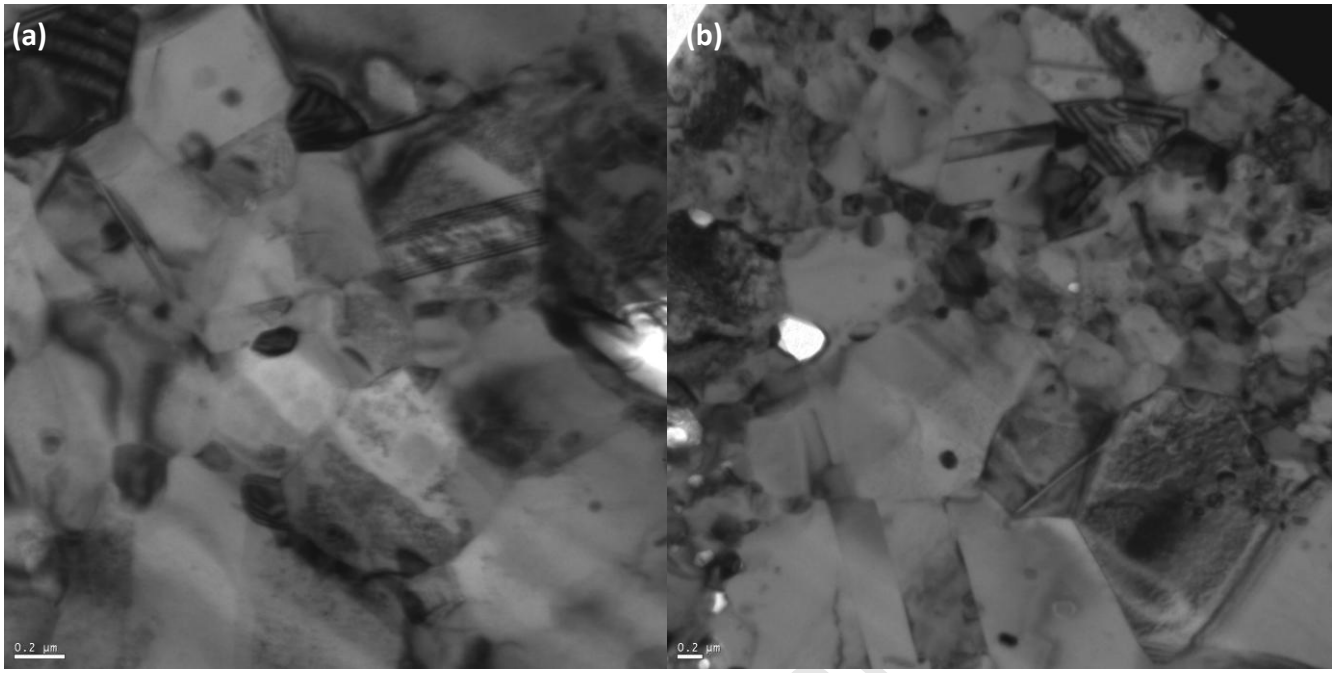

Fig. 3: (a) and (b) Bright field TEM images of the microstructure of the as-HIPed sample.

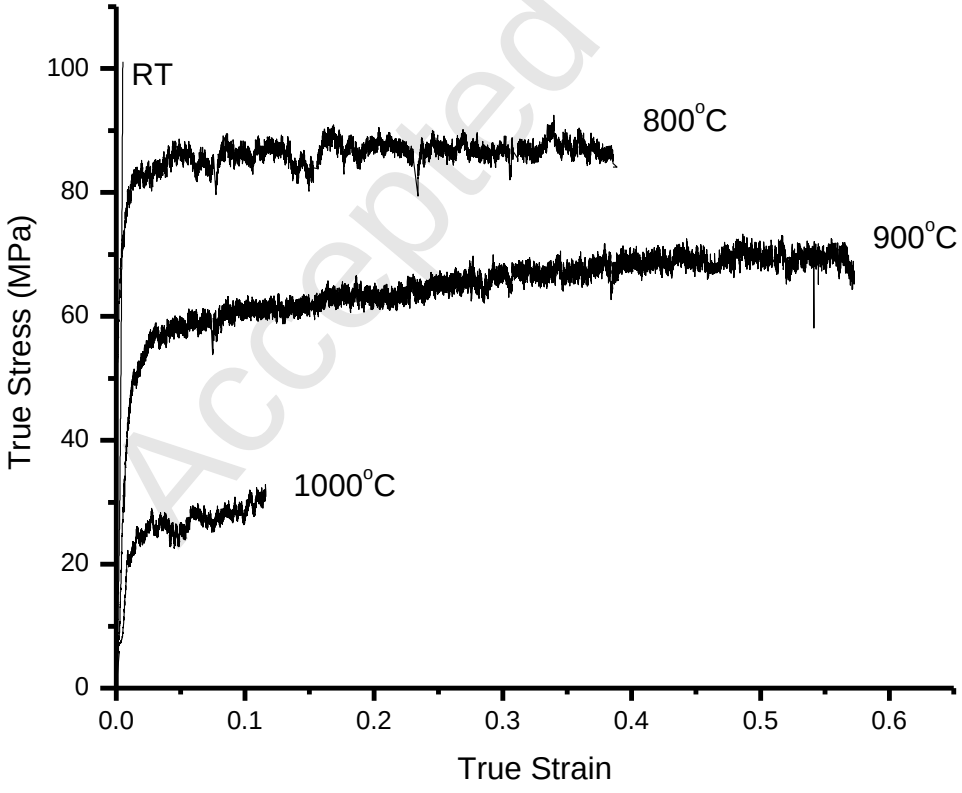

Fig. 4: Tensile true stress-true strain curves of the specimens tensile tested at (a) room temperature (b) 800°C (c) 900° C (d) 1000°C.

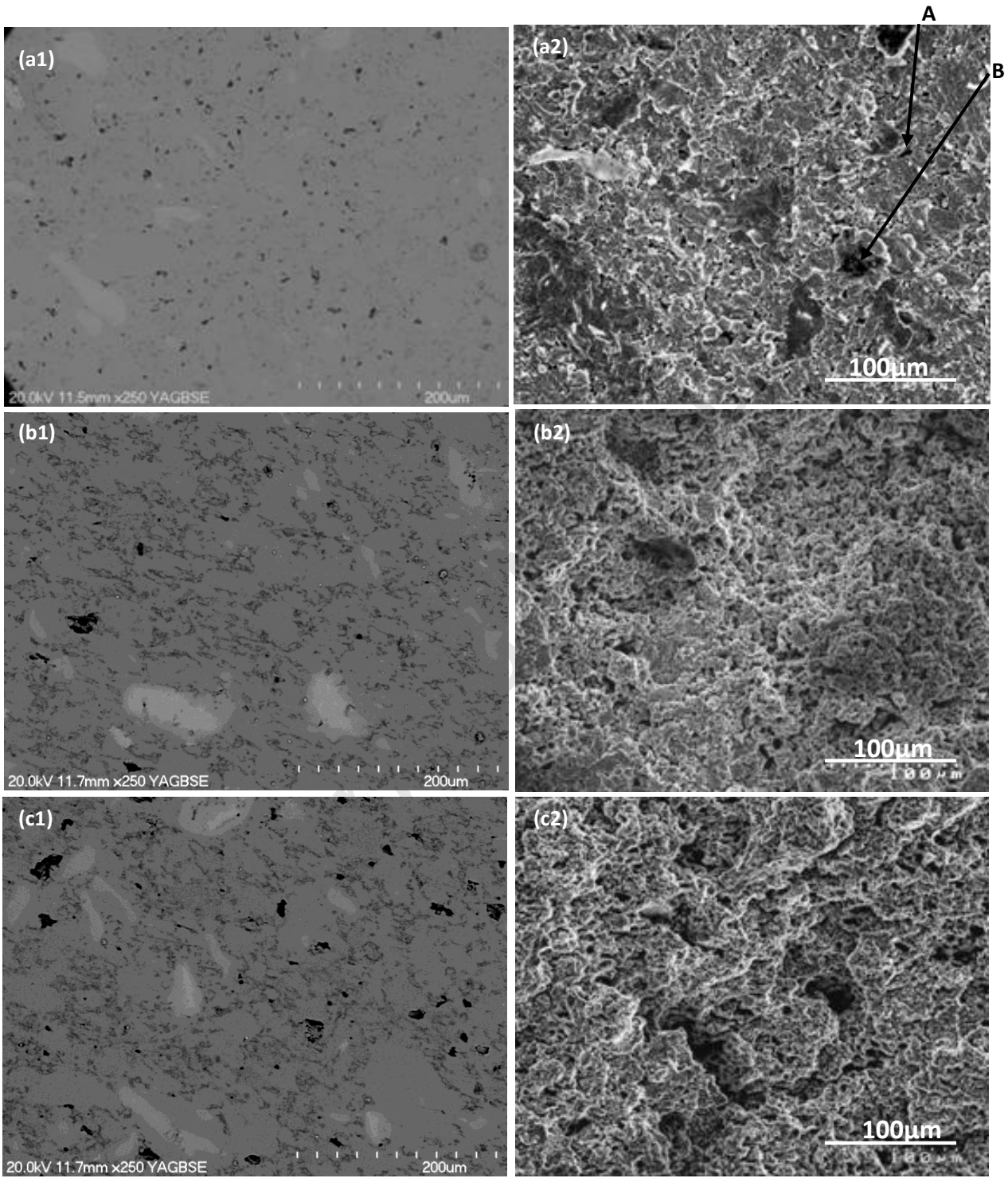

Fig. 5: SEM backscattered electron images of the longitudinal sections (within gauge length) ((a1), (b1) and (c1) and corresponding SEM secondary electron images of the fracture surfaces of the tensile tested specimens ((a2), (b2) and (c2)) tested at different temperatures: (a1) and (a2) room temperature; (b1) and (b2) 800^{o}C; and (c1) and (c2) 900^{o}C.

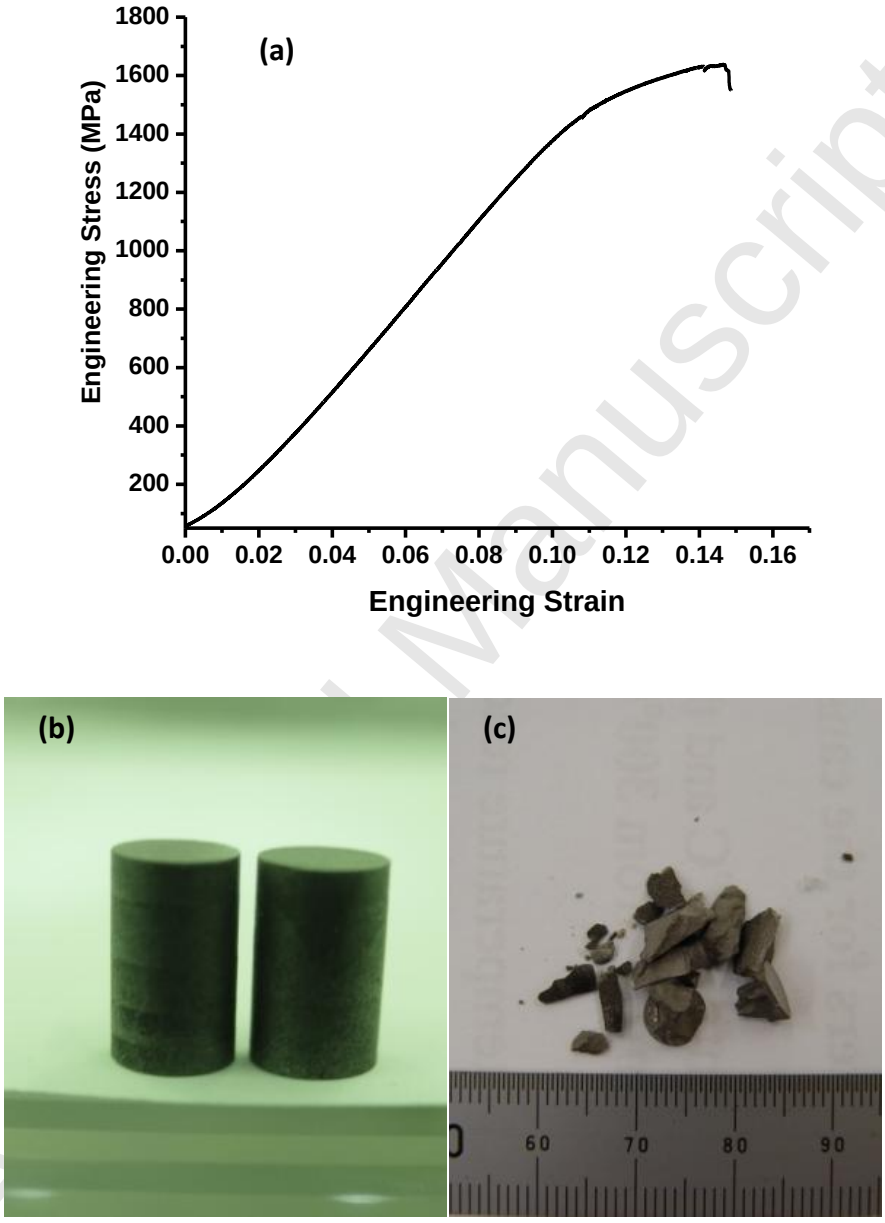

Fig. 6: (a) The compressive true stress-true strain curve of a specimen tested at room temperature; (b) image of the specimens used for room temperature compression testing; and (c) fractured pieces after room temperature compression testing.

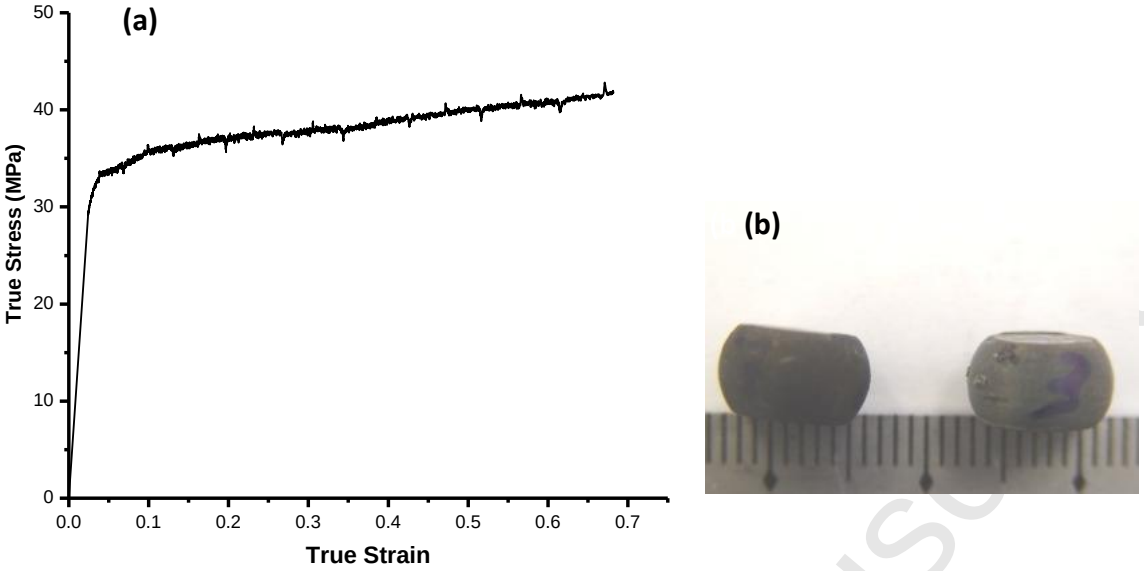

Fig. 7: (a) The compressive true stress-true strain curve of a specimen, tested at 900^{o}C; (b) specimens after compression testing at 900^{o}C.

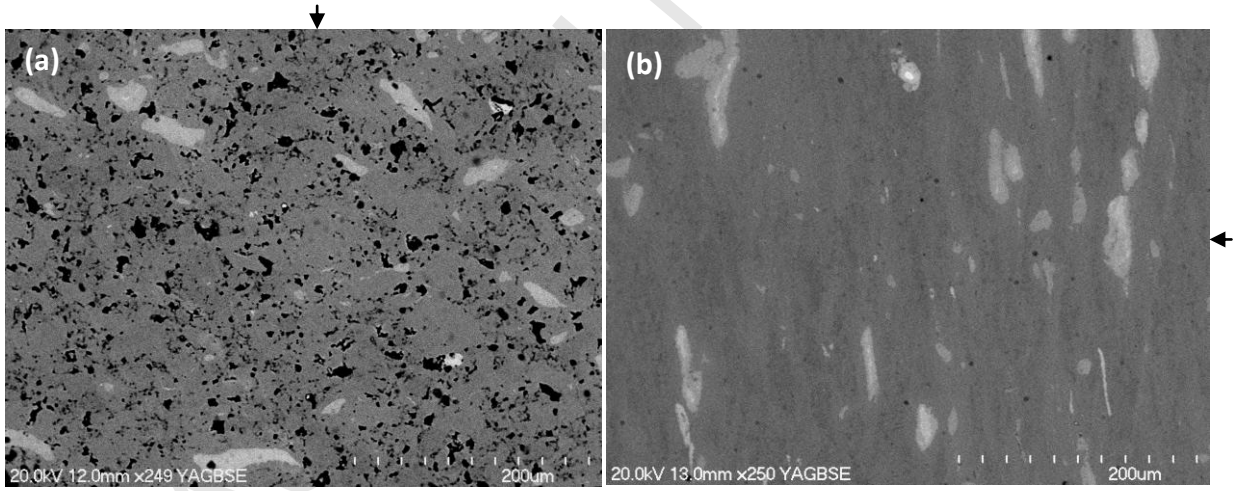

Fig. 8: Images of the cross sections of the specimens after compression testing at (a) room temperature and (b) 900^{o}C (arrows indicate direction of the compressive force)

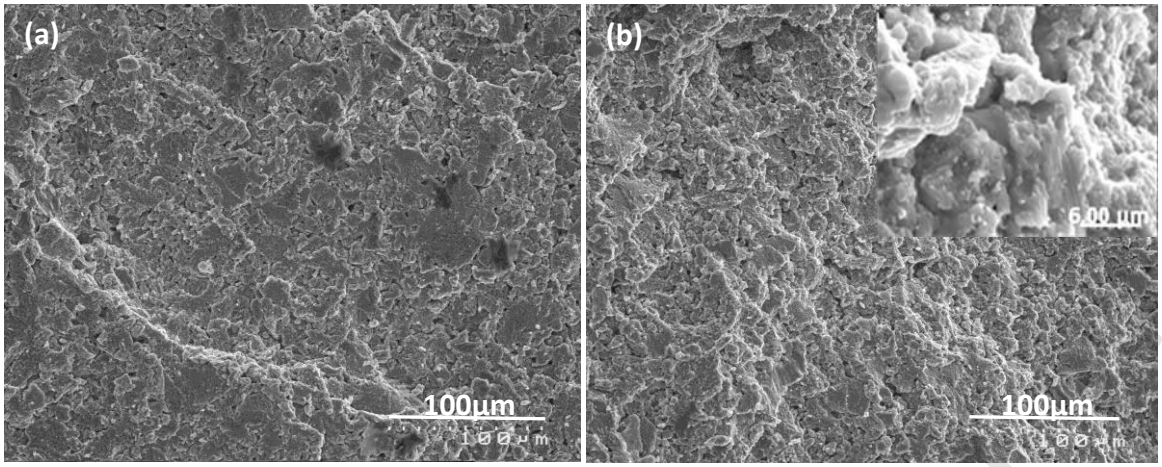

Fig. 9: Fractured surfaces of the specimens after RT compression testing, showing (a) quasi cleavage type of fracture; (b) quasi cleavage with a few regions showing ductile fracture behaviour; (c) a region of ductile fracture.

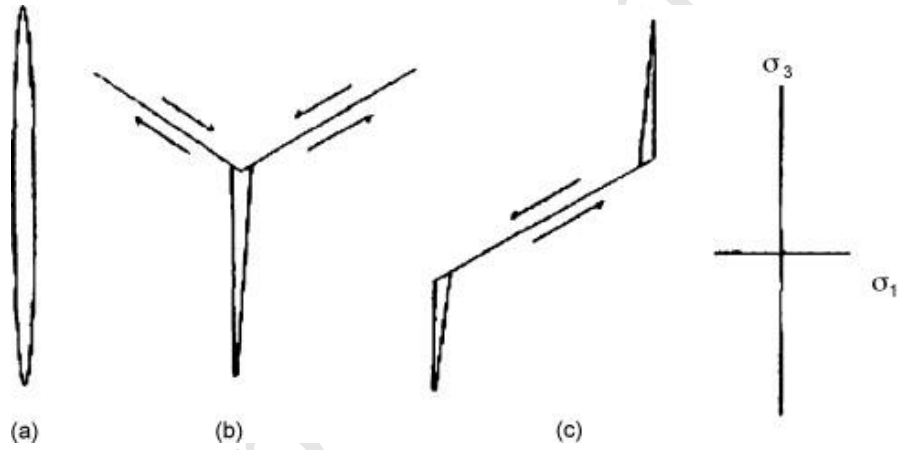

Fig. 10: Crack initiation and propagation paths in compression loading mode [17, 18]

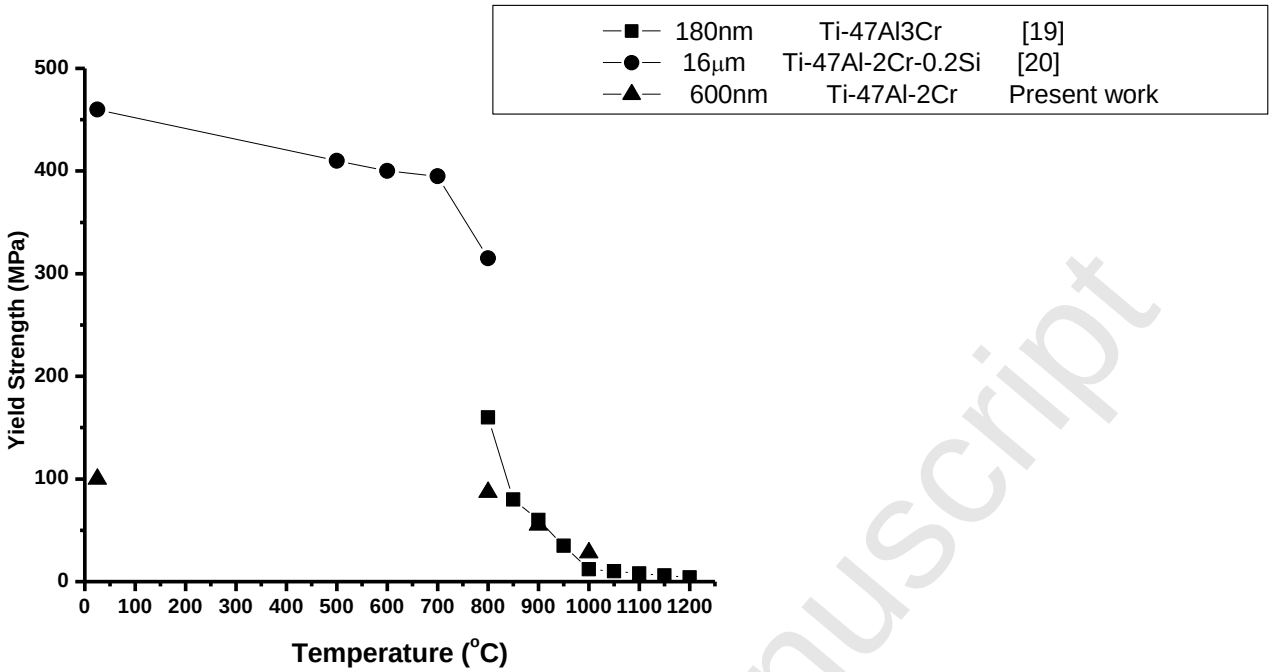

Fig. 11: Comparison of yield strength in tension of TiAl based alloy samples of similar compositions at different temperatures.

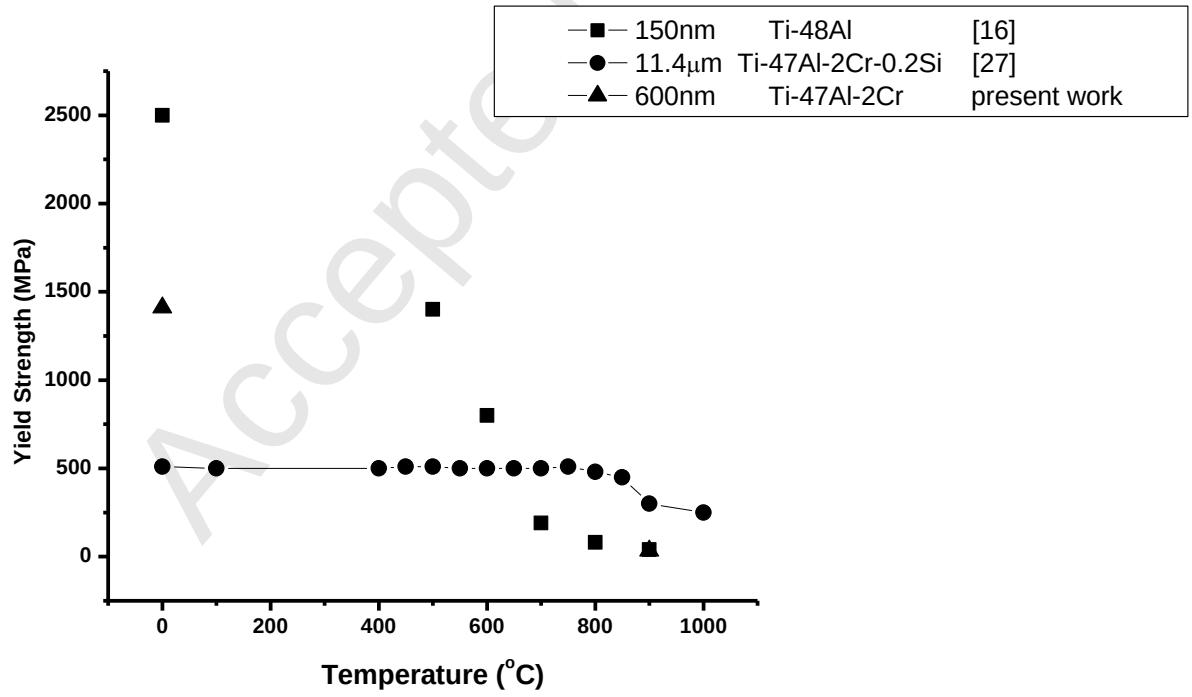

Fig. 12: Comparison of yield strength in compression of TiAl based alloy samples of similar compositions at different temperatures.